VCAM-1 expression on dystrophic muscle vessels has a critical role in the recruitment of human blood–derived CD133$^+$ stem cells after intra-arterial transplantation

Manuela Gavina, Marzia Belicchi, Barbara Rossi, Linda Ottoboni, Fabio Colombo, Mirella Meregalli, Maurizio Battistelli, Laura Forzenigo, Piero Biondetti, Federica Pisati, Daniele Parolini, Andrea Farini, Andrew C. Issekutz, Nereo Bresolin, Franco Rustichelli, Gabriela Constantin, and Yvan Torrente

Recently our group demonstrated the myogenic capacity of human CD133$^+$ cells isolated from peripheral blood when delivered in vivo through the arterial circulation into the muscle of dystrophic *scid/mdx* mice. CD133$^+$ stem cells express the adhesion molecules CD44, LFA-1, PSGL-1, α4-integrins, L-selectin, and chemokine receptor CCR7. Moreover these cells adhere in vitro to VCAM-1 spontaneously and after stimulation with CCL19. Importantly, after muscle exercise, we found that the expression of VCAM-1 is strongly up-regulated in dystrophic muscle vessels, whereas the number of rolling and firmly adhered CD133$^+$ stem cells significantly increased. Moreover, human dystrophin expression was significantly increased when muscle exercise was performed 24 hours before the intra-arterial injection of human CD133$^+$ cells. Finally, treatment of exercised dystrophic mice with anti–VCAM-1 antibodies led to a dramatic blockade of CD133$^+$ stem cell migration into the dystrophic muscle. Our results show for the first time that the expression of VCAM-1 on dystrophic muscle vessels induced by exercise controls muscle homing of human CD133$^+$ stem cells, opening new perspectives for a potential therapy of muscular dystrophy based on the intra-arterial delivery of CD133$^+$ stem cells. (Blood. 2006;108: 2857-2866)

Introduction

Attempts to repair muscle damage in patients with Duchenne muscular dystrophy (DMD) by transplanting myogenic progenitors directly into muscles are hampered by the problem of cell survival and the limited migration of these cells in the muscles. The delivery of myogenic stem cells to the sites of muscle lesions through the systemic circulation is a potential alternative approach to treat this disease, but injected cells may become trapped intravenously in other organs (eg, liver, spleen, lung) so that only a small portion enters the muscle microvasculature and migrates to dystrophic muscle. Our recent work supports the idea that stem cells can reach the site of muscle regeneration and can contribute to muscle repair and to replenishment of the satellite cell pool after intra-arterial injection, suggesting that this technique might be particularly suited for treating muscle dystrophy.[1,2] This protocol succeeded primarily because of the widespread distribution of donor stem cells through the muscle capillary network, a distinct advantage of this strategy over previous approaches. Elucidation of the mechanisms involved in the muscle homing of stem cells will aid the development of a potential therapy for muscular dystrophy based on the systemic delivery of stem cells. It has been shown recently that VLA-4–VCAM-1 interactions efficiently mediate rolling and arrest in vivo in blood vessels from bone marrow or under pathologic conditions characterized by an activated endothelium.[3-5] In the present study, we focused our attention on the molecular mechanisms involved in human CD133$^+$ cells homing to dystrophic muscle and efficiently mediating their transplantation.

Materials and methods

Isolation and characterization of human blood–derived CD133$^+$ cell fraction for FACS analysis

Human circulating CD133$^+$ cells were isolated from blood mononucleated cells, as previously described.[1] The enrichment of CD133$^+$ cells was followed by a second round of cell sorting for the CD133 antigen with a dual-laser FACSVantage SE (Becton Dickinson, Franklin Lakes, NJ). Sorted CD133$^+$ cells were double labeled with anti–CD133-phycoerythrin (anti–CD133-PE) (Miltenyi Biotech, Bergisch Gladbach, Germany), anti–VLA4-FITC, anti–CD44-FITC, anti–LFA1-FITC, anti–L-selectin–FITC (BD Pharmingen, San Diego, CA), anti–PSGL1-FITC (MBL International, Woburn, MA), anti–CCR3-FITC, anti–CCR5-FITC, anti–CCR7-FITC, anti–CXCR3-FITC, and anti–CXCR4-FITC (R&D Systems, Minneapolis, MN). Isotype control was performed using fluorescein isothiocyanate

From the Stem Cell Laboratory, Department of Neurological Sciences, Fondazione Istituto di Ricovero e Cura a Carattere Scientifico (IRCCS), Ospedale Maggiore Policlinico, Centro Dino Ferrari, University of Milan, Italy; the Department of Pathology, Division of General Pathology, University of Verona, Italy; the Fondazione IRCCS Ospedale Maggiore Policlinico, Institute of Nuclear Medicine, Milan, Italy; the Radiology Unit, Fondazione IRCCS Ospedale Maggiore Policlinico of Milan, Italy; the Department of Pediatrics, Pathology, and Microbiology-Immunology, Dalhousie University, Halifax, NS, Canada; and the Department of Sciences Applied to Complex Systems, Polytechnic University of Marche, Ancona, Italy.

Submitted April 24, 2006; accepted June 15, 2006. Prepublished online as *Blood* First Edition Paper, June 29, 2006; DOI 10.1182/blood-2006-04-018564.

Supported by the Association Française contre les Myopathies; the Italian Ministry of Health (Ricerca Finalizzata); the IRCCS Fondazione Policlinico Hospital (Progetto a Concorso); Cariverona Foundation; Fondo Incentivazione Ricerca di Base (FIRB); and Fondazione Italiana Sclerosi Multipla (FISM).

Reprints: Yvan Torrente, Department of Neurological Science, University of Milan, Padiglione Ponti, Ospedale Policlinico, via Francesco Sforza 35, 20122 Milan, Italy; e-mail: yvan.torrente@unimi.it.

The publication costs of this article were defrayed in part by page charge payment. Therefore, and solely to indicate this fact, this article is hereby marked "advertisement" in accordance with 18 U.S.C. section 1734.

(FITC)–conjugated mouse IgG_1, R-phycoerythrin (R-PE)–conjugated rat IgG_{2a}. To ensure the quality of our analysis, we also investigated sorted $CD133^-$ cells for the expression of molecules, as previously indicated. We also characterized the adhesion molecules and chemokines receptor expression of sorted $CD133^+$ cells after stimulation with 5 ng TNF-α in RPMI 1640 medium (Gibco, Invitrogen, Carlsbad, CA) enriched with insulin, 20 ng/mL epidermal growth factor (EGF), and 10 ng/mL basic fibroblastic growth factor (bFGF). The cells were analyzed 4 to 5 hours after stimulation and after overnight incubation with TNF-α.

In vitro adhesion assay on ICAM-1 and VCAM-1

We evaluated the functionality of LFA-1 and VLA-4 expressed by $CD133^+$ cells using an in vitro spontaneous adhesion assay for human ICAM-1 and VCAM-1 (R&D Systems).[6] After isolation, sorted $CD133^+$ cells were resuspended in PBS, $CaCl_2$, $MgCl_2$ 1 mM, and 10% FCS (pH 7.2) at 2.5×10^6/mL, and 25 μL of this suspension was plated on 18-well glass slides for 30 minutes. The slides were coated with recombinant 1 μg/mL ICAM-1 and 1 μg/mL VCAM-1 (R&D Systems), as previously described.[6] Five microliters of CCL19/MIP3β (R&D Systems) was added (1 μM) to the cell-containing wells for 3 minutes at 37°C. This chemokine has been shown to induce the adhesion of human lymphocytes to endothelial cells or endothelial cell adhesion ligands. Cells were fixed in 1.5% glutaraldehyde for 20 minutes. The number of adherent cells in a 0.2-mm^2 field was counted using cell-counting software.

Selectin chimera binding assays

The functionality of PSGL-1 expressed on sorted blood-derived $CD133^+$ and $CD133^-$ cells was demonstrated with a cytofluorimetric assay. Approximately 5×10^5 cells were resuspended in 100 μL standard medium (SM [DMEM, 0.1% BSA, 0.1% NaN_3]) and were incubated for 30 minutes at 4°C with E- and P-selectin chimeras (R&D Systems). Cells were washed twice, resuspended in 100 μL SM, and incubated with anti–human IgG FITC (diluted 1:32; Sigma, St Louis, MO) for 20 minutes at 4°C. After 2 washes in SM, cells were pelleted and resuspended in fresh DMEM immediately before FACS analysis. Nonspecific staining was established by the addition of EDTA (10 mM) to staining reactions conduced with the selectin chimeras.

In vivo staining of endothelial adhesion molecules

To characterize the adhesion molecules expressed by murine muscle vessels, we analyzed 3 groups (n = 5 each) of 3-month-old *scid/mdx* mice: group 1, mice under basal conditions; group 2, mice 4 to 5 hours after stimulation with 1 μg TNF-α injected intravenously; group 3, mice after muscle stress from 1 hour of swimming and analysis of adhesion molecule expression 24 hours later. Monoclonal antibodies (mAbs) anti–E-selectin (RME-1), anti–P-selectin (RMP-1), anti–MAdCAM-1 (MECA-367), anti–ICAM-1 (YN1.1.7.4), anti–VCAM-1 (M.K.2.7), and isotype-matched control antibodies were labeled using the Alexa Fluor 568 labeling kit (Molecular Probes, Eugene, OR). Striate muscle vessels were visualized using intravital microscopy, as described.[1] Intravital visualization of the Alexa Fluor 568 (Molecular Probes) staining was confirmed by fluorescence analysis of the cryosectioned hind limbs of each treated animal. Immunocytochemistry for the expression of CD31 and αSMA was also carried out to identify venules and arterioles, respectively. Intravital microscopy images were captured with a BXW0WI microscope (Olympus, Tokyo, Japan) equipped with an Olympus Achroplan water immersion objective (20×/0.5 NA; focal distance, 3.3 mm).

Intravital microscopy

With the intravital microscopy model,[7] we verified the muscle homing and vascular adhesion properties of $CD133^+$ stem cells into the pectoral and iliopsoas muscles of *scid/mdx* mice after muscle exercise (n = 6) and after administration of anti–VCAM-1 mAb (n = 6). Animals were anesthetized, and the pectoral muscle was analyzed with an intravital microscope (BX50WI; Olympus, Tokyo, Japan). A dextran dye (155 kDa; Sigma) was injected to visualize the blood vessels. $CD133^+$ stem cells (10^6) were fluorescently labeled with green CMFDA (5-chloromethylfluorescein diacetate; Molecular Probes) and injected by a digital pump at flow rate of 0.13 to 1 μL/s.

Characterization of muscle homing of $CD133^+$ stem cells by HMPAO labeling

We tested the muscle selectivity of human circulating $CD133^+$ cells by labeling them with technetium Tc 99m-labeled hexamethylpropylene amine oxime (HMPAO), a radioactive marker previously described.[8] Cells were incubated for 2 hours at 37°C in RPMI medium supplemented with 1 μCi/mL (0.037 MBq) HMPAO. Labeling efficiency was measured with a dose calibrator (Atomlab 100; Biodex Medical, Shirley, NY). Cell vitality was assessed by trypan blue and by double staining with propidium iodide (PI) and annexin V. HMPAO-labeled $CD133^+$ (10×10^5) or $CD133^-$ cells were injected into the right femoral artery of 2-month-old *scid/mdx* mice in basal condition (n = 5 each) and after swimming (n = 5 each). We compared the distribution of radioactivity of the first series of experiments with animals pretreated intraperitoneally with 250 μg selective blocking antibodies against VCAM-1 (n = 4) and ICAM-1 (n = 4) (generous gifts from Eugene C. Butcher, Laboratory of Immunology and Vascular Biology, Department of Pathology, Stanford University School of Medicine, Stanford, CA) 1 hour before stem cell injection. Animals were killed 24 hours later, tissue from muscle, lung, kidney, liver, and brain was collected, and radioactive content was measured in a β-counter (LS1801; Beckman Coulter, Hialeah, FL) as previously described.[8]

Microfil perfusion

PkH2-labeled $CD133^+$ cells (5×10^5) were injected into the right femoral artery of *scid/mdx* mice in basal conditions (n = 3) and 24 hours after exercise (n = 3). After cell injection, the mice were perfused with 10 mL PBS and then 10 mL liquid silicon rubber (Microfil; Flow Tech, Carver, MA). Hind limbs of treated mice were isolated in toto and placed under refrigeration at 4°C overnight to allow polymerization. On the following day, specimens were carefully dissociated and placed in a 50% mixture of water and glycerin. At successive 24-hour intervals, the glycerin concentration was raised to 75%, then to 85%, and finally to pure glycerin. Statistical analysis using the Student *t* test was also performed. Immunofluorescence images were captured with a DMIRE2 microscope (Leica Microsystems, Cambridge, United Kingdom) and a Leica DC350 camera. The microscope was equipped with a 40×/0.75 NA dry objective. Images were acquired and processed with Leica Qfluoro software.

Labeling of $CD133^+$ cells with iron oxide

To better characterize the migratory capacity of $CD133^+$ cells in mouse dystrophic animal models, we used live cell tracking methods such as magnetic resonance imaging (MRI) after labeling with nanoparticles of iron oxide (Endorem; Guerbet, Sulzbach, Germany).[9,10] Human $CD133^+$ stem cells were labeled with 250 μg/mL Endorem (Guerbet) in RPMI 1640 medium enriched with 20 ng/mL EGF and 10 ng/mL bFGF for 12 or 24 hours. We tested different cell suspensions (100 000, 50 000, 20 000, 5000, 500 cells) in 1.7% gelatin. For in vivo experiments, $CD133^+$ cells were injected intra-arterially in the *scid/mdx* dystrophic animal model and were visualized with MRI. Images were obtained using a 4.7-T spectrometer (Burker, KooWeeRup, VIC, Australia) equipped with a surface coil made in house. Single sagittal, coronal, and transversal images were obtained by a fast gradient-echo sequence to localize the subsequent T_2-weighted transverse images, as measured by a standard turbo spin-echo sequence. The same muscles monitored by MRI were isolated and characterized by immunohistochemistry for the expression of CD133 antigen and Prussian blue staining.[9]

Histochemistry and immunocytochemistry of injected dystrophic muscles

For human dystrophin detection, unexercised (n = 5) and exercised (n = 6) *scid/mdx* mice were injected intra-arterially with 500 000 human $CD133^+$

stem cells, as previously described.[1] Sixty days later, muscle sections were characterized using the anti–human nuclear lamin A/C (Novocastra, 1:200), anti–human dystrophin (1:50; Chemicon, Temecula, CA), anti–α-smooth muscle actin (DAKO, Carpinteria, CA), and anti-CD31 (1:100; Chemicon) antibodies, as previously described.[1]

Results

Characterization of adhesion molecules and chemokine receptors

To evaluate the migratory capacity of human circulating CD133$^+$ cells, we first studied by flow cytometry the adhesion molecules and chemokine receptors expressed on their surfaces. In these experiments, we sorted CD133$^+$ and CD133$^-$ cells, and we characterized both populations by flow cytometry analysis. Sorted CD133$^+$ cells (99% ± 1% [mean ± SD]) coexpressed CD44 and LFA-1. In particular, we observed 2 subpopulations of CD133 on the basis of LFA-1^{dim} and LFA-1^{bright} expression. In addition, 83% ± 2% of sorted CD133$^+$ cells expressed PSGL-1, 44% ± 3% expressed VLA-4, and 60% ± 5% expressed L-selectin. Chemokine receptor analysis showed very low expression of CXCR3 and CXCR4 (4% ± 3%), whereas 44% ± 5.4% of CD133$^+$ cells were positive for CCR7. Less than 2% of sorted CD133$^+$ cells expressed CCR3 (1.6% ± 1.3%) or CCR5 (1.7% ± 1.5%). We observed that sorted CD133$^-$ cells expressed 98% ± 1% CD44, 87% ± 1% LFA-1, 63.5% ± 1% L-selectin, 53.5% ± 1% CCR7, 19% ± 1% CXCR3, 3.5% ± 1% CXCR4, 1.2% ± 1% CCR3, and 0.09% ± 1% CCR5. In contrast to CD133$^+$ cells, very low expression of VLA-4 (0.6% ± 0.5%) and reduced expression of PSGL-1 (7.5% ± 1%) were observed on sorted CD133$^-$ cells. Although the expression of chemokine receptors and adhesion molecules was regulated in leukocytes by the inflammatory microenvironment, human circulating CD133$^+$ cells did not seem to be particularly influenced by this condition. In fact, after 5 and 20 hours of stimulation with TNF-α in culture medium, only the percentage of cells expressing L-selectin was decreased from 60% to 4%. The other adhesion molecules and chemokine receptors showed no modification in their expression as a result of exposure to TNF-α (Figure 1). All these data demonstrate that human CD133$^+$ cells express a complete pattern of adhesion molecules and chemokine receptor CCR7, an important molecule usually involved in the activation and migration of leukocytes under physiologic and pathologic conditions.

Evaluation of adhesion capability of CD133$^+$ cells in vitro

The adhesion capacity of CD133$^+$ cells to integrin ligands was evaluated in vitro by adhesion assays to VCAM-1 and ICAM-1 before and after stimulation with MIP3β (CCL19, a ligand for CCR7 receptor). Rapid adhesion assays showed that CD133$^+$ cells spontaneously adhered to VCAM-1 and ICAM-1, suggesting that VLA-4 and LFA-1 integrins expressed on CD133$^+$ cells were, in part, already activated and able to bind their counter ligands without chemoattractant stimulation. Interestingly, the number of cells spontaneously adherent to VCAM-1 was 178 ± 28, which was more than 10 times greater than the number of cells that adhered to ICAM-1 (15.7 ± 3.1), showing that nonactivated CD133$^+$ cells displayed higher binding activity of VLA-4 than LFA-1. Stimulation with MIP3β improved significantly the number of adherent cells to VCAM-1, and, though the number of adherent cells remained low, an increase was also observed in ICAM-1 (Figure 2A). Taken together, these results suggest that

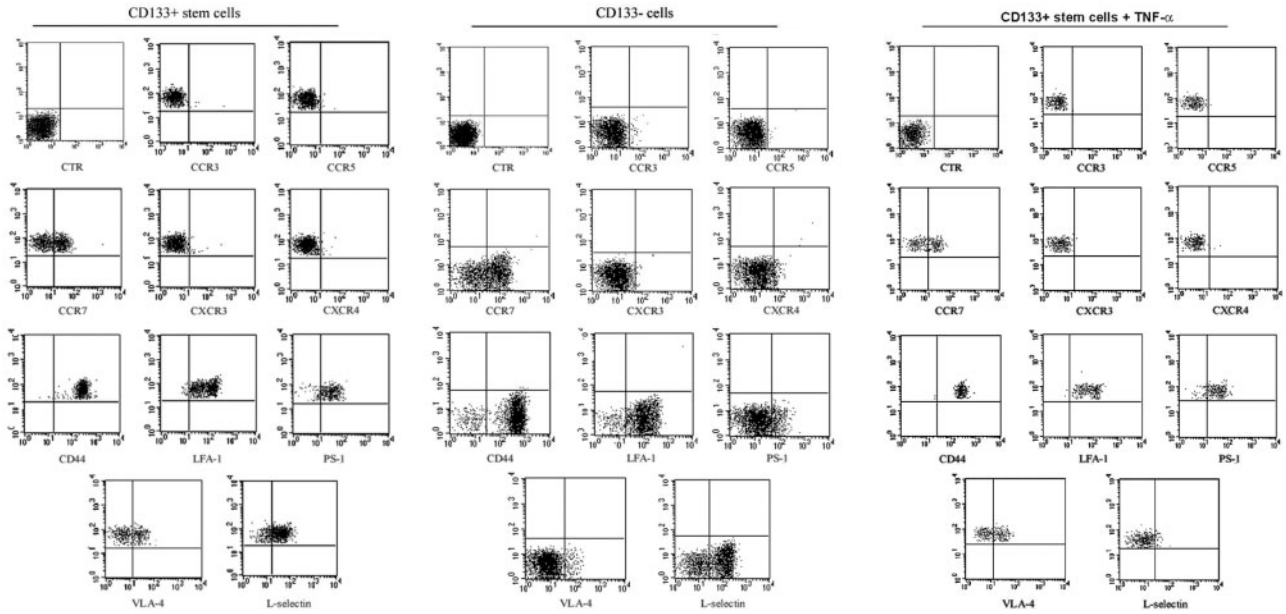

Figure 1. FACScan immunophenotyping of sorted human circulating CD133$^+$ and CD133$^-$ cells. Human circulating CD133$^+$ cells obtained from the peripheral blood of healthy donors were characterized after FACSVantage sorting for the expression of adhesion molecules and chemokine receptors. The expression of the adhesion molecules was also evaluated in sorted CD133$^-$ cells and after stimulation of sorted CD133$^+$ cells with 5 ng/mL TNF-α. CD133$^+$ cells (99% ± 1%) coexpressed CD44 and LFA-1. In particular, we observed 2 subpopulations of CD133 on the basis of LFA-1^{dim} and LFA-1^{bright} expression. In addition, 83% ± 2% of CD133$^+$ cells expressed PSGL-1, 44% ± 3% expressed VLA-4, and 60% ± 5% expressed L-selectin. Analysis of chemokine receptors showed a very low expression of CXCR3 and CXCR4 (4% ± 3%), whereas 44% ± 5.4% of CD133$^+$ cells were positive for CCR7. Less than 2% of total CD133$^+$ cells expressed CCR3 (1.6% ± 1.3%) or CCR5 (1.7% ± 1.5%). We observed that sorted CD133$^-$ cells expressed 98% ± 1% CD44, 87% ± 1% LFA-1, 63.5% ± 1% L-selectin, 53.5% ± 1% CCR7, 19% ± 1% CXCR3, 3.5% ± 1% CXCR4, 1.2% ± 1% CCR3, and 0.09% ± 1% CCR5. Very low expression of VLA-4 (0.6% ± 0.5%), CCR3 (1.2% ± 1%), and CCR5 (0.09% ± 1%) was observed. After cytokine stimulation of sorted CD133$^+$ cells, the expression of L-selectin decreased from 60% to 4%. The other adhesion and chemokine molecules showed similar decreases.

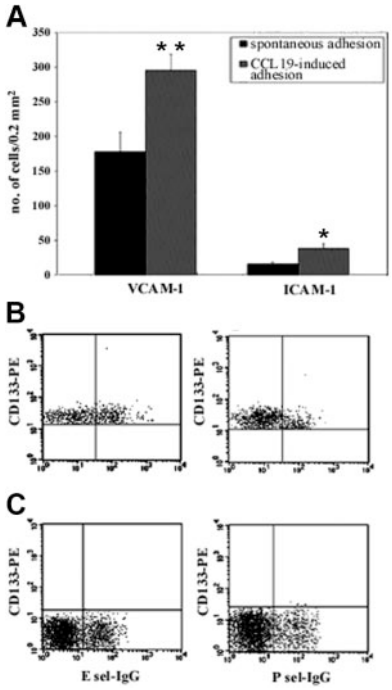

Figure 2. CD133$^+$ cells express functional adhesion molecules and CCR7 receptor. We evaluated the functionality of adhesion molecules expressed by CD133$^+$ cells with in vitro adhesion assays on their ligands, and we tested the effect of chemokines on this binding (A). Unstimulated CD133$^+$ cells adhered to human VCAM-1 in vitro. This binding was improved by stimulation with CCR7 ligand MIP3β. Only a reduced number of cells adhered to human ICAM-1, and a chemokine response to stimulation led to increased cell adhesion. Adhesion was completely absent in uncoated wells and extremely low in wells coated with FCS (background adhesion). Results are expressed as mean ± SD of adherent cells per 0.2 mm^2. The number of spontaneously adhered cells was compared with the number of cells that adhered after stimulation with CCL19 by using 2-tailed Student *t* test. $^*P < .01$; $^{**}P < .001$. The functionality of PSGL1 was evaluated with a cytofluorimetric assay; 40% of CD133$^+$ cells were able to bind E-selectin, but only 10% were able to bind *P*-selectin (B). CD133$^-$ showed very low ability to bind E- and P-selectin (1.1% ± 0.3% and 1.9% ± 0.2%, respectively) (C).

CD133$^+$ cells preferentially adhere in vitro using VLA-4 integrin. To demonstrate specificity, the assays were performed in the presence of anti–VCAM-1 and anti–ICAM-1 antibodies (R&D Systems), and the blockade of binding was greater than 95% (data not shown). We also performed flow cytometry assays using E- and P-selectin chimeras on the sorted CD133$^+$ and CD133$^-$ fractions of blood-derived mononucleated cells. Results demonstrated that approximately 40% of human CD133$^+$ cells bound to E-selectin, whereas approximately 10% of these cells bound to P-selectin. These results suggested that unstimulated CD133$^+$ cells expressed functional ligands mainly for E-selectin (Figure 2B). Moreover, the binding of CD133$^-$ cells for E- and P-selectin was, respectively, 1.1% ± 0.3% and 1.9% ± 0.2% (Figure 2C), showing that these cells displayed low binding activity of PSGL-1.

In vivo staining of adhesion molecules in dystrophic vessels

To support the results obtained with binding assays, we performed an in vivo staining study aimed at identifying the endothelial adhesion molecules potentially involved in dystrophic muscle homing. For this reason, *scid/mdx* mice were monitored in basal conditions (n = 5), after 1 hour of swimming exercise (n = 5), and after intravenous injection of 1 μg TNF-α (n = 5). Through the use of fluorescent antibodies and intravital microscopy, we observed that vessels of 3-month-old *scid/mdx* mice were positive for the expression of P-selectin, whereas MAdCAM-1, ICAM-1, and E-selectin were not detected. Positivity for anti–ICAM-1 and anti–MAdCAM-1 antibodies was found in Peyer patches, as expected. P-selectin–positive vessels were visible in pectoral and hind limb muscles with tortuous morphology and regions of narrowing, and very low expression of VCAM-1 was observed in some vessels. After stimulation with TNF-α and 24 hours after muscle exercise, no variation in the expression of E-selectin and MAdCAM-1 was observed, whereas VCAM-1 in vivo staining showed an increase in the number of positive vessels and an enhanced intensity of the positive vessels (Figure 3). Surprisingly, and in contrast to the VCAM-1 results, ICAM-1 expression was not up-regulated in dystrophic muscle after TNF-α injection, though in the same animals we found positivity for ICAM-1 in Peyer patches and brain. No detectable differences were observed between arteriolar and venular staining. In vivo staining performed with a control mAb anti–human Ras showed no in vivo staining of dystrophic muscle (data not shown). In vivo staining data were confirmed by immunofluorescence for CD31 and αSMA performed on cryosections of perfused mice. It was, in fact, possible to detect several CD31$^+$ muscle venules and αSMA-positive arterioles that coexpressed P-selectin or VCAM-1 (Figure 3) in the cryosections obtained from the same muscles previously monitored by in vivo staining.

Intravital microscopy performed in dystrophic muscle vessels

Muscle homing and vascular adhesion properties of CD133$^+$ cells were next verified in the pectoral and gastrocnemius muscles of 3-month-old *scid/mdx* mice under flow conditions. For all in vivo experiments, we used blood-derived CD133$^+$ cells obtained with magnetic column separation. Even if the purity obtained with this method was just greater than 90%, the contaminating fraction of CD133$^-$ cells did not affect our results. In fact, the characterization of adhesion molecules and the adhesion assays of sorted CD133$^-$ cells showed a low capacity of these cells to interact with the main endothelial adhesion molecules involved in the recruitment from the bloodstream described in our experiments. When injected into the aortic arch (through the right carotid), few human CD133$^+$ cells were able to firmly adhere to the murine muscle vessels, but most interacting cells performed rolling (21 ± 5.4 for rolling interactions and 0.8 ± 0.3 for firm adhesion; mean ± SEM). We observed that some cells were mechanically trapped in blood capillaries and in proximity to narrowing vessels. This low capacity of CD133$^+$ cells to firmly adhere to the dystrophic vessel endothelium probably resulted because the expression of P-selectin, as a rolling receptor, in the muscle vessels of *scid/mdx* was insufficient to mediate adhesion interactions necessary for efficient firm arrest. We thus extended these experiments injecting the CD133$^+$ cells in *scid/mdx* mice, which, after 1 hour of swimming exercise, displayed increased expression of VCAM-1. Rolling events were more frequent (increase of 50%; $P < .04$) in vessels stimulated with exercise than in vessels in basal condition (31.5 ± 3.6) (Figure 4E). We also analyzed the quality and strength of rolling by measuring the rolling velocities (Vrolls) of interacting human CD133$^+$ cells (Figure 4F). Median Vroll in basal conditions and after swimming was 49.9 μm/s and 24.9 μm/s, respectively. In addition, the distribution of Vroll in velocity classes showed a larger number of cells with higher Vroll under basal conditions, suggesting that different molecular mechanisms might mediate rolling interactions after swimming compared with basal conditions. Importantly, we observed a 6-fold increase in the number of

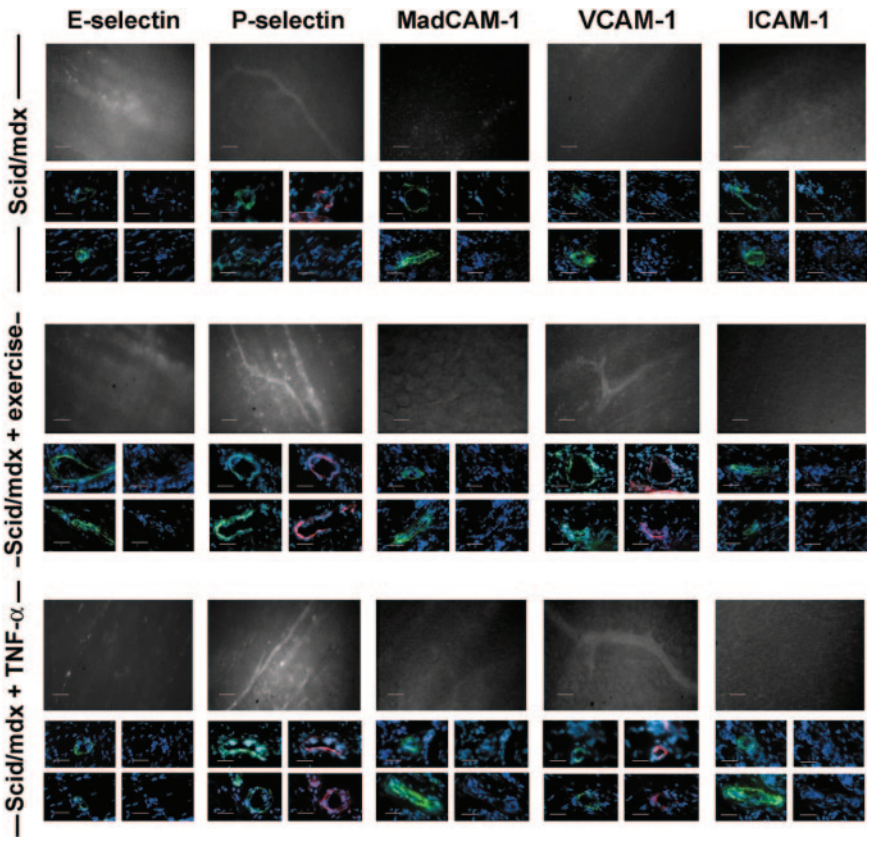

Figure 3. Characterization of endothelial adhesion molecules in *scid/mdx* mice. Adhesion molecule expression on the endothelium of dystrophic muscle was evaluated with the use of in vivo staining followed by observation with intravital microscopy and on cryosections before and after TNF-α stimulation or muscle exercise. Fluorescein-protein (F/P) ratios for mAbs were 3.0 for anti–E- and anti–P-selectin mAbs, 3.2 for anti–ICAM-1 mAb, 2.9 for anti–MAdCAM-1 mAb, and 3.4 for anti–VCAM-1 mAb. An anti–human Ras mAb was used as control and had an F/P ratio of 3.6 (data not shown). Murine vessels of *scid/mdx* mice expressed P-selectin in basal condition as shown by in vivo staining. Moreover, after muscle exercise and TNF-α stimulation, we registered significant improvement in the number of vessels expressing P-selectin and VCAM-1. In vivo staining data were confirmed by immunofluorescence staining showing the expression of P-selectin or VCAM-1 (in red) but not E-selectin, MadCAM-1, or ICAM-1 in $CD31^+$ venules (shown in the middle line of each condition), αSMA–positive arterioles (shown in the lower line of each condition), or murine muscle vessels (both in green). DAPI-positive nuclei are shown in blue. Vessels were acquired at ×40 magnification. Scale bars represent 100 μm for intravital microscopy (black-and-white images) and 10 μm for immunostaining (color images).

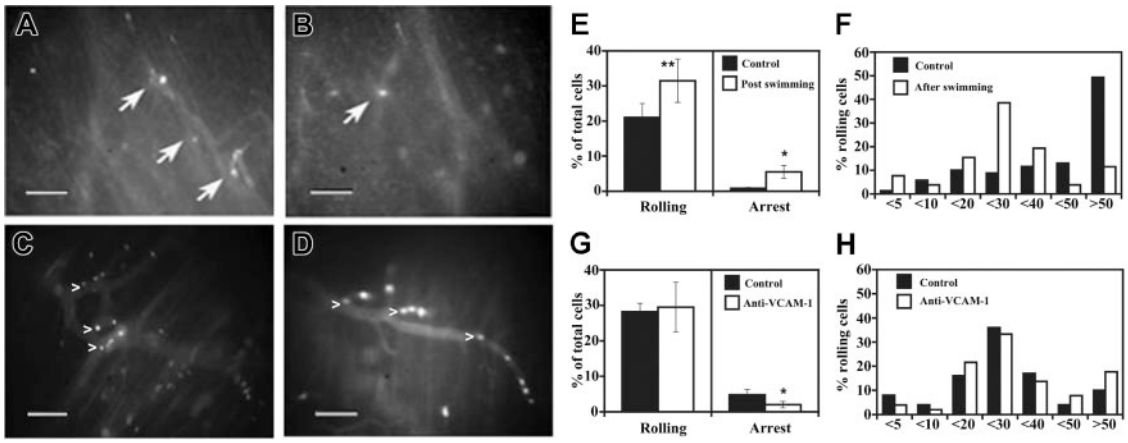

Figure 4. Intravital microscopy. Human circulating $CD133^+$ cells injected in the dystrophic *scid/mdx* mice firmly adhered in dystrophic muscle vessels (A-D). To improve contrast between the intravascular and extravascular compartment, the animals were injected intravenously with low doses of FITC-dextran. Labeled cells (bright dots indicated by arrows) can be seen in muscle vessels a few minutes after intra-arterial injection under basal conditions (A-B). After muscle exercise, it was possible to observe significant improvement in the number of cells (white dots) that firmly adhered in venules of different diameters and apparently also in capillaries of *scid/mdx* mice (C-D). The behavior of fluorescently labeled $CD133^+$ cells was studied under basal conditions and after swimming (E). Ten venules per 4 animals were studied under basal conditions, and 8 venules per 4 animals were studied after swimming. Data are expressed as mean ± SEM. Hemodynamic parameters (mean ± SD) are as follows: D = 46 ± 11 μm; Vm = 872 ± 42 μm/s; WSR = 157 ± 33 s^{-1}; WSS = 3.9 ± 0.8 (dyn/cm^2) in mice studied under basal conditions and D = 37 ± 13 μm; Vm = 810 ± 56 μm/s; WSR = 177 ± 44 s^{-1}; WSS = 4.4 ± 0.9 (dyn/cm^2) in mice studied after swimming. Velocity histograms were generated by measuring rolling velocity (F). Frequency distributions were calculated after cells were assigned to velocity classes from greater than 0 μm/s to 5 μm/s, 5-10 μm/s, 10- 20 μm/s, and so on. To quantify the enhancement of rolling induced by overexpression of VCAM-1 by muscle vessels, we evaluated the behavior of $CD133^+$ cells in the same animal on the same vessel in 2 steps: after exercise and after treatment with anti–VCAM-1. Cells were injected before anti–VCAM-1 mAb administration (G). Then mice received 100 μg mAb intravenously, and, after 10 minutes, we injected the same number of cells as for the control. Five venules were examined per 3 mice. Bars depict rolling and arrest fractions as percentages of control cells that rolled and arrested in the same venule. Data are expressed as the mean ± SEM. Groups were compared by using 2-tailed Student *t* test. Hemodynamic parameters (mean ± SD) were D = 28.7 ± 7 μm; Vm = 599 ± 177 μm/s; WSR = 174 ± 69 s^{-1}; WSS = 4.3 ± 1.7 (dyn/cm^2) during the injection of control cells and D = 28.7 ± 7 μm; Vm = 555 ± 87 μm/s; WSR = 161 ± 50 s^{-1}; and WSS = 4 ± 1.2 (dyn/cm^2) after injection of anti–VCAM-1 mAb. (H) Velocity histograms before mAb administration and after anti–VCAM-1 mAb injection were generated as in panel F. Scale bars represent 100 μm. $^*P < .01$; $^{**}P < .04$.

CD133$^+$ cells able to firmly adhere in capillaries, small postcapillary venules, and larger venules (5.5 ± 1.9) (Figure 4E). The increased recruitment after swimming could be explained by the natural capacity of CD133$^+$ cells to bind VCAM-1 because of the presence on their membrane of the integrin very late antigen (VLA-4). Taken together, these results show that the activation of dystrophic vessel endothelium by exercise improves the adhesion of human CD133$^+$ cells in vivo.

We next sought to identify the molecular mechanisms of rolling and arrest in dystrophic muscle venules after swimming. Rolling interactions were not inhibited after the administration of anti–VCAM-1 mAb. In contrast, almost 60% of firm adhesion/arrest was blocked by the use of anti–VCAM-1 mAb (Figure 4G). Median Vroll was 23.8 for control cells and 24.5 after anti–VCAM-1 administration. However, though not statistically significant, the mean ± SD value of Vroll was slightly increased after VCAM-1 blockade: 31 ± 21 for control cells compared with 39 ± 42 after mAb blockade. In addition, the distribution of Vroll in velocity classes showed a slightly larger number of cells with higher Vroll after the administration of anti–VCAM-1 mAb (Figure 4H), suggesting that VCAM-1 might contribute to roll strengthening of some CD133$^+$ cells. An isotype-matched control antibody (anti–human Ras) had no effect on rolling or arrest (data not shown). These results clearly show an important role for VCAM-1 in the recruitment of CD133$^+$ cells in dystrophic muscle after muscle exercise. Hemodynamic parameters for intravital microscopy experiments are depicted in Figure 4E,G.

Detection of intra-arterially injected CD133$^+$ stem cells by fluorescence and microfil perfusion

To confirm the results obtained by intravital microscopy and quantify firmly adhered cells with a different method, animals injected intra-arterially with CD133$^+$ stem cells were perfused with microfil. This technique offers the possibility of eliminating transient adhered cells, observing the 3-dimensional cast of dystrophic muscle vessels, and identifying injected cells distribution in toto.

In basal conditions, the transillumination of microfil-perfused vessels of intra-arterially injected *scid/mdx* mice rarely showed PKH2 CD133$^+$-labeled cells in large and small vessels of dystrophic muscles (2 ± 1.41 cells/field at 20× magnification) (Figure 5A, C). In contrast, after muscle exercise, we observed a 4- to 5-fold increase of the number of adhered cells in large vessels and distributed in the capillary network (10 ± 2.51 cells/field at 20× magnification; $P < .01$) (Figure 5B, D-E).

MRI analysis

To test the migration capacity of human circulating CD133$^+$ stem cells and to monitor the fate of implanted cells using a noninvasive method such as MRI, we labeled these cells with a contrast agent based on dextran-coated superparamagnetic iron oxide nanoparticles clinically approved as a blood pool agent (Endorem; Guerbet). In vitro results demonstrated that CD133$^+$ stem cell iron incorporation leads to MRI visualization. The iron oxide nanoparticles in cultured CD133$^+$ stem cells were observed as blue spots after Prussian blue staining (Figure 6F-G). Cell counting of Prussian blue–stained cells revealed that after

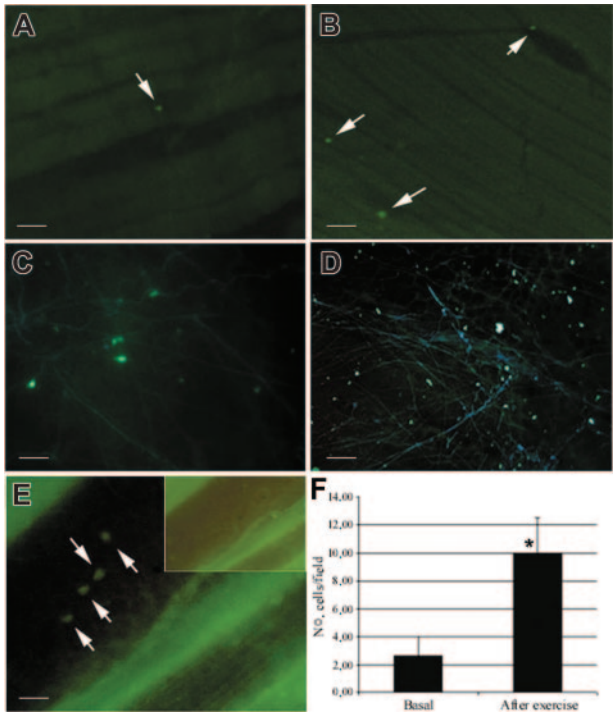

Figure 5. Evaluation of the effect of muscle exercise on the recruitment of human CD133$^+$ cells. CD133$^+$ stem cells were incubated with PkH2 green to allow detection by fluorescence microscopy with a perfusion technique that showed the vasculature in 3 dimensions. Intra-arterially injected CD133$^+$ stem cells were rarely found in the vessels of dystrophic muscles before exercise (A, C). In contrast, after swimming exercise intra-arterially injected *scid/mdx* mice showed an increased number of adhered cells in the capillary network (B, D) and to large vessels (E). (E) Large vessels perfused with a rubber silicon fluid were detected in transillumination. (inset) Cells were not evident in other fluorescence acquisitions, confirming that positively registered cells in vessels were not artefacts. (F) Statistical evaluation by Student *t* test of the number of CD133$^+$ cells adhered to the vessel and confirmed significant improvement in recruitment after exercise. *$P < .05$. Scale bars represent 100 μm (A-C), 200 μm (D), and 25 μm (E). In panels A-E, arrows indicate the labeled cells. Error bars in panel F indicate standard deviation.

12 hours of labeling with Endorem (Guerbet), the percentage of labeled cells was 44.2% ± 7.4% and that after 24 hours of labeling, the percentage was increased to 85.6% ± 8.3%. Longer labeling did not increase either the number of labeled cells or the number of iron particles inside the cells. A colorimetric assay for the quantification of cell proliferation and cell viability based on the cleavage of the tetrazolium salt WST-1 (Roche Molecular Biochemicals, Indianapolis, IN) by mitochondrial dehydrogenases in viable cells did not show any differences between nanoparticle-labeled and nonlabeled cell groups. Moreover, MRI images showed a clear hypointense signal at all concentrations of more than 500 cells (Figure 6A-E). At 24 hours after intra-arterial transplantation, we observed a hypointense signal obtained by MRI evaluation in the quadriceps, tibialis anterior, and soleus muscle tissues. No recognizable hypointense signal in the muscle of uninjected leg was detected. The hypointense signal in muscle remained visible during the first 24 hours after intra-arterial injection with no change in shape. The histology of these hypointense areas showed that a large number of Prussian blue–positive cells had entered into the muscle and that most of them coexpressed the CD133 antigen around vessels, suggesting migration from the arterial circulation (Figure 6I, J).

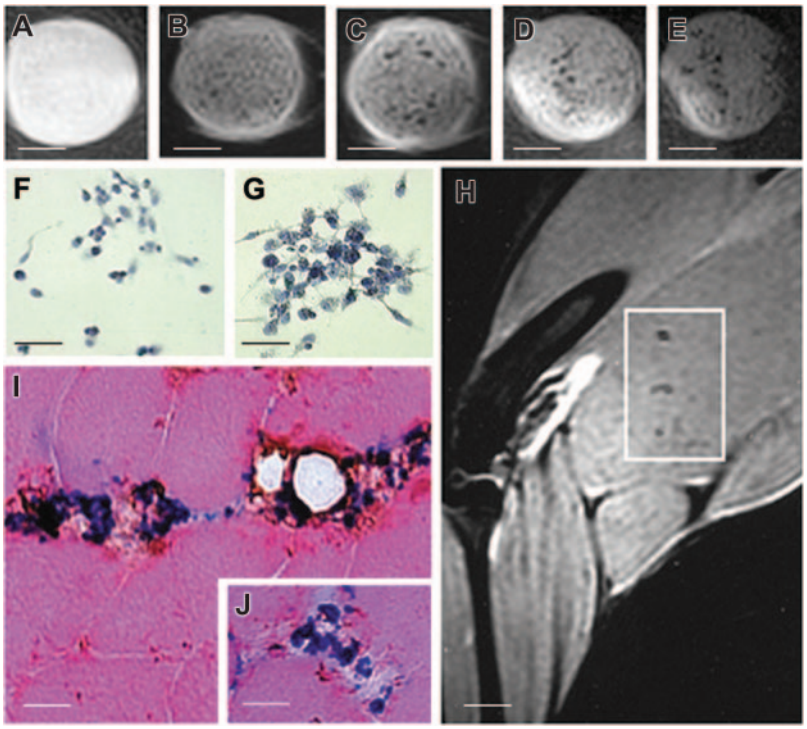

Figure 6. T2-weighted images of phantoms and injected muscle leg tissues and implanted CD133$^+$ stem cells. MR images of phantoms formed by a set of test tubes containing a suspension of Endorem-labeled cells in gelatin: (A) 500, (B) 5000, (C) 20 000, (D) 50 000, and (E) 100 000 cells. Sample contains gelatin only. Inhomogeneities in the phantom images were caused by the moderate sedimentation of cells while the gelatin was setting. Sequence parameters were repetition time (TR), 2000 msec; effective echo time (TE), 42.5 msec; turbo factor, 4; number of acquisitions (AC), 16; field of view (FOV), 3.5 cm; matrix, 256 × 256; slice thickness, 0.5 mm; slice separation, 1 mm. Two sets of interleaved transversal images were measured to cover the whole muscle. For in vitro experiments, phantoms of sterile agarose 2% containing labeled cells were measured by a similar sequence with different geometry: FOV, 6 cm; matrix, 256 × 256; slice thickness, 1 mm. Only one slice was measured for phantoms. Prussian blue staining of samples containing 50 000 (F) and 100 000 (G) cells. (H) Several areas of hypointense signal were seen 24 hours after intra-arterial grafting by MRI (white quadrant). (J) Histologic examination performed on biopsy specimens of MRI-positive areas confirmed positive Prussian blue–stained cells that coexpressed the CD133 antigen around muscle vessels. Scale bars represent 100 μm (A-E); 25 μm (F-G, I, inset); 3 mm (H).

In vitro labeling of CD133$^+$ stem cells with ^{99m}Tc-labeled HMPAO and evaluation of labeled cell accumulation in dystrophic *scid/mdx* mice

To test the efficiency of labeling, CD133$^+$ stem cells were incubated with 15 MBq HMPAO in serum-free RPMI between 30 and 120 minutes. A time-dependent incorporation of HMPAO was observed with maximum efficiency after 60 minutes, resulting in an overall labeling efficiency of 61% ± 11%. Next, we investigated whether the labeling affected cell viability or function. Up to 120 hours after HMPAO labeling, trypan blue uptake in the radiolabeled CD133$^+$ stem cells was not significantly different from that in controls, with 97.1% ± 2.1% of cells trypan blue negative after labeling (n = 3). The viability of labeled CD133$^+$ cells was also confirmed by cytofluorimetric analysis. In fact, annexin V and PI staining showed a vitality of 97% ± 2% (Figure 7A). Similarly, the functional capacity of CD133$^+$ stem cells to migrate in response to vascular endothelial growth factor in a modified Boyden chamber assay was not affected by radiolabeling when radiolabeled CD133$^+$ stem cells were compared with their unlabeled controls (data not shown). To determine the leakage of HMPAO into the supernatant, we checked the activity of HMPAO in the supernatants and in the adherently growing CD133$^+$ stem cells. We found that 32.4% ± 5.2% of the HMPAO incorporated into CD133$^+$ stem cells was retained after 24 hours (data not shown). We thus investigated the distribution of radioactively labeled human CD133$^+$ stem cells after their intra-arterial injection into *scid/mdx* mice. In these experiments, we compared the distribution of radioactivity obtained after the injection of CD133$^+$ cells in exercised mice pretreated with anti–ICAM-1 (n = 4) or anti–VCAM-1 (n = 4) or without pretreatment (n = 5). As control, we characterized the radioactivity distribution obtained after intra-arterial injection of radiolabeled CD133$^-$ cells in basal condition (n = 5) and after exercise (n = 5). Twenty-four hours after the injection of CD133$^+$ cells, a high tracer accumulation was found in muscle tissues of mice without pretreatment (70.1% ± 18.3% of the injected activity). The muscle tracer distribution did not show major changes after anti–ICAM-1 mAb pretreatment (71.2% ± 9.1% of whole body activity). However, we observed reduced accumulation of CD133$^+$ cells in other organs, such as the spleen, in which it is known that the blood vessel endothelium expresses ICAM-1. In contrast to the results obtained with anti–ICAM-1 antibody, we registered a marked reduction (approximately 10-fold) of the radioactivity in the muscle of dystrophic mice pretreated with anti–VCAM-1 mAb (Figure 7B). The specific radioactivity in isolated muscles after swimming exercise and no pretreatment compared with anti–ICAM-1 pretreatment were, respectively, 68 047.9 ± 5048.36 cpm/g tissue and 90 337.1 ± 6874.11 cpm/g tissue. After anti–VCAM-1 pretreatment, specific total muscle activity decreased significantly to 8152.4 ± 1507.36 cpm/g ($P < .05$). All these data suggest a critical role of VCAM-1 in the recruitment of CD133$^+$ stem cells in exercised dystrophic muscle tissues. However, an important interaction was observed in control mice injected with CD133$^-$ cells. In fact, the radioactivity detected after the injection of these labeled cells was 79 721.5 ± 1060.66 cpm/g tissue in basal condition, whereas a decrement of 3-fold (to 31 533 ± 1342.07 cpm/g tissue) was observed after exercise. These data demonstrate that the improvement observed in the recruitment of radiolabeled cells after swimming exercise is related to the CD133$^+$ fraction, and these observations are not affected by the contaminating negative cells.

Human dystrophin expression in injected *scid/mdx* mice

We then investigated the in vivo ability of CD133$^+$ stem cells to differentiate into the myogenic lineage after intra-arterial injection. As shown by radioactivity studies to contain donor cells,

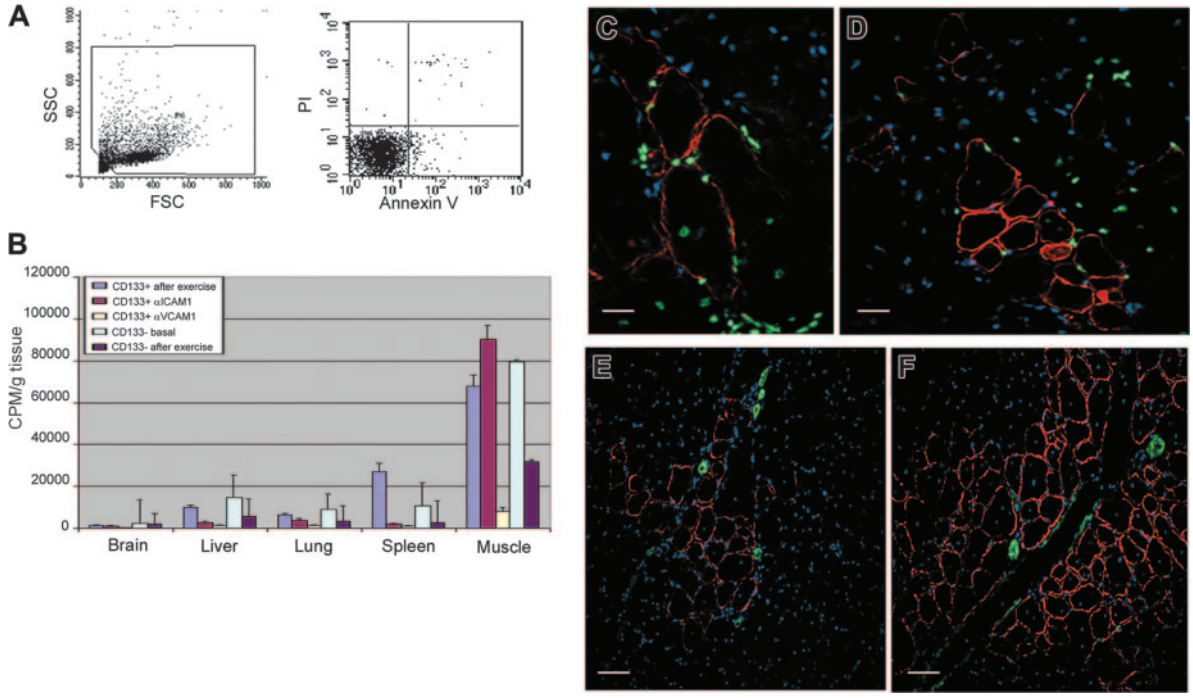

Figure 7. HMPAO-labeled CD133$^+$ cells and measurement of the distribution of radioactivity by γ-counter in dystrophic injected mice. (A) Viability of radiolabeled cells. Flow cytometry analysis with PI and annexin V confirmed the 97% viability observed with trypan blue staining. (B) When we blocked the VCAM-1 molecule with the anti–VCAM-1 antibody, we obtained a significant decrease in radioactivity 12 hours after intra-arterial injection in the muscles and in the different organs, such as brain, lungs, kidneys, spleen, and liver, compared with values obtained from untreated *scid/mdx* mice. A decrement in radioactivity in organs of mice treated with anti–ICAM-1 was also detected, whereas in the muscle we registered a significant improvement in counts per minute per gram. Animals injected with CD133$^-$ cells used as control showed a decrement in the recruitment of intra-arterial injected cells after exercise (C-F). Human dystrophin expression 60 days after intra-arterial injection of human CD133$^+$ stem cells is shown. Error bars indicate standard deviation. (C-D) Colocalization of the human dystrophin (red), human lamin A/C nuclei (green), and Hoechst (blue) demonstrated the formation of normal human myofibers in dystrophic muscles after transplantation of the human blood–derived CD133$^+$ cells. The number of human dystrophin–positive myofibers in quadriceps of exercised mice (D, F) was higher than muscle of unexercised mice (C, E). Low magnification revealed mature human dystrophin muscle fibers (red) near αSMA-positive muscle arteries (green) after the intra-arterial transplantation of CD133$^+$ stem cells into unexercised (E) and exercised (F) dystrophic *scid/mdx* mice. Scale bars represent 100 μm (C), 75 μm (D), and 50 μm (E-F).

tissues were evaluated for the expression of human dystrophin 2 months after CD133$^+$ stem cell engraftment. Human dystrophin–positive myofibers were counted in 5 nonadjacent cross-sections of the intra-arterially injected muscles, and the longitudinal dimension of the positive area was approximately 600 μm. In unexercised animals that received intra-arterial injection, we observed that the highest number of dystrophin-positive fibers per cross-section was detected in the quadriceps muscle of the injected leg (roughly 0.5% to 1.0% of total fibers in a given cross-section) (Figure 7E; Table 1). However, after muscle swimming/exercise, the percentage of human dystrophin increased 4-fold in all observed muscle tissues of the injected leg (Figure 7F; Table 1). In all injected muscles, many of the human dystrophin–positive fibers expressed the anti–human lamin A/C (Figure 7C-D). Moreover, human dystrophin–positive myofibers were clustered primarily near αSMA-positive muscle arteries (Figure 7E-F). Indeed, positive human lamin A/C cells were found near the human dystrophin–positive myofibers. All these data suggest that muscle exercise increases the number of mature myofibers expressing the human dystrophin after the intra-arterial transplantation of blood-derived CD133$^+$ stem cells.

Discussion

Recently we demonstrated that human circulating cells expressing the CD133 antigen behave as a stem cell population capable of commitment to hemopoietic, endothelial, and myogenic lineages.[1] The discovery of the mechanisms involved in the muscle homing of stem cells will aid in improving a potential therapy for muscular dystrophy based on the systemic delivery of such stem cells.

Almost all CD133$^+$ cells coexpressed CD44 and LFA-1, with a particular distribution of the latter antigen in 2 subpopulations, LFA-1^{dim} and LFA-1^{bright}, suggesting the existence of a less activated and a more activated subpopulation of CD133$^+$ cells. More than 40% of the CD133 cells expressed PSGL-1, VLA-4, L-selectin, and CCR7, suggesting that part of CD133$^+$ cells might migrate in secondary lymphoid organs.[11] Moreover, the expression of these chemokine receptors and adhesion molecules of CD133$^+$ cells do not seem to be particularly influenced by exposure to TNF-α. All these data demonstrate that freshly isolated human CD133$^+$ cells already express a pattern of adhesion molecules potentially able to mediate migration through the blood vessel wall. Thus, we investigated the ability of stem cells to bind endothelial adhesion molecules such as ICAM-1, VCAM-1, P-selectin, and E-selectin using in vitro functional assays. The results obtained suggest that VLA-4 and LFA-1 integrins expressed by CD133$^+$ cells are functional, at least in part, and are able to spontaneously bind VCAM-1 and ICAM-1, respectively. However, we observed that the capacity of VLA-4 to bind VCAM-1 was more than 10-fold higher than the capacity of LFA-1 to bind ICAM-1, suggesting that CD133$^+$ cells might preferentially migrate using VLA-4. In addition, unstimulated CD133$^+$ cells express functional ligands for

Table 1. Blood-derived CD133$^+$ cells yield human Dys3$^+$ myofibers within injected dystrophic muscles after intra-arterial transplantation of unexercised and exercised *scid/mdx* mice

	Quadriceps		Soleus		Tibialis anterior	
Positive myofibers	**Unexercised**	**Exercised**	**Unexercised**	**Exercised**	**Unexercised**	**Exercised**
Mouse 1						
Lamin A/C$^+$	11 ± 3	45 ± 1*	7 ± 5	52 ± 3*	4 ± 2	32 ± 1*
Dys$^+$ fibers/s	26 ± 13	73 ± 5*	14 ± 9	61 ± 10*	10 ± 2	55 ± 11*
Dys/lamin A/C$^+$ fibers	15 ± 61	45 ± 1*	9 ± 6	47 ± 7*	5 ± 8	32 ± 22*
Mouse 2						
Lamin A/C$^+$	10 ± 8	35 ± 10	15 ± 2	21 ± 14	7 ± 3	37 ± 5*
Dys$^+$ fibers/s	12 ± 5	59 ± 9*	9 ± 2	48 ± 11*	18 ± 11	91 ± 32*
Dys/lamin A/C$^+$ fibers	9 ± 3	45 ± 4*	3 ± 1	27 ± 12*	9 ± 7	72 ± 18*
Mouse 3						
Lamin A/C$^+$	24 ± 11	101 ± 17*	10 ± 7	70 ± 24*	17 ± 4	33 ± 13
Dys$^+$ fibers/s	16 ± 11	68 ± 11*	6 ± 2	49 ± 16*	14 ± 10	46 ± 7*
Dys/lamin A/C$^+$ fibers	8 ± 3	44 ± 12*	3 ± 1	31 ± 21*	8 ± 2	29 ± 13*
Mouse 4						
Lamin A/C$^+$	19 ± 6	36 ± 19	8 ± 5	24 ± 8	15 ± 7	53 ± 11*
Dys$^+$ fibers/s	10 ± 6	61 ± 21*	4 ± 3	41 ± 13*	9 ± 8	57 ± 31*
Dys/lamin A/C$^+$ fibers	7 ± 4	51 ± 15*	1 ± 2	35 ± 20*	2 ± 1	31 ± 16*
Mouse 5						
Lamin A/C$^+$	18 ± 9	81 ± 21*	10 ± 4	72 ± 12*	11 ± 4	43 ± 23*
Dys$^+$ fibers/s	20 ± 11	89 ± 22*	9 ± 1	53 ± 12*	14 ± 11	61 ± 15*
Dys/lamin A/C$^+$ fibers	7 ± 3	67 ± 19*	5 ± 3	26 ± 8*	5 ± 3	37 ± 25*

Results are expressed as number of human lamin A/C-, Dys-, and Dys/lamin A/C-positive cells per section of muscle tissue (± SD) in a longitudinal dimension of approximately 600 μm.

Dys indicates dystrophin.

*$P < .01$.

E-selectin, but not for P-selectin, suggesting preferential binding to E-selectin during rolling interactions in vivo. Using intravital microscopy, it was possible to characterize the expression of murine endothelial adhesion molecules potentially involved in dystrophic muscle homing. Unexpectedly, some blood vessels of *scid/mdx* mice in basal conditions were positive for the expression of P-selectin, whereas MAdCAM-1, ICAM-1, and E-selectin were not detected. Very low expression of VCAM-1 was detected on some vessels. Moreover, when injected into the circulation of *scid/mdx* mice, few human circulating CD133$^+$ cells were able to firmly adhere to the murine muscle vessels. In fact, CD133$^+$ cells bind only E-selectin, but not P-selectin, chimera, whereas dystrophic muscle vessels express P-selectin but not E-selectin. This lack of matching between endothelium and CD133$^+$ cells may explain the low capacity of stem cells to interact with the blood vessel wall in dystrophic muscles. P- and E-selectin on endothelial cells are primary adhesion molecules for capture and the initiation of rolling.[12] E- and P-selectin rolling was previously described for hematopoietic progenitor cells (HPCs) in bone marrow vessels.[3] Selectin-independent rolling of HPCs can be also mediated by α4-integrins, which interact with endothelial VCAM-1.[3] However, constitutive expression of P-selectin and very low expression of VCAM-1 in some dystrophic vessels were not sufficient to mediate efficient recruitment of CD133$^+$ cells in our experimental models. After treatment of animals with TNF-α or after swimming muscle exercise, E-selectin and MAdCAM-1 expression were not up-regulated in dystrophic muscle vessels, whereas a massive increase in the expression of VCAM-1 was observed. Surprisingly, and in contrast to VCAM-1 data, ICAM-1 expression was not up-regulated in dystrophic muscle, though in the same animals we found positivity for anti–ICAM-1 mAb in Peyer patches and brain.[4] Abnormal P-selectin expression in dystrophic muscle and the lack of ICAM-1 and E-selectin up-regulation after TNF-α administration support the hypothesis that dystrophic muscle might represent a unique milieu able to selectively recruit blood cells expressing peculiar combinations of adhesion molecules. Intravital microscopy performed in the dystrophic vessels of *scid/mdx* mice, enriched in VCAM-1 and P-selectin after exercise, showed an increase in the number of cells able to roll and firmly adhere. The lack of E-selectin expression on *scid/mdx* endothelium and the lack of binding of P-selectin chimera by CD133$^+$ cells suggest that rolling events and firm arrest of human stem cells in dystrophic muscle vessels might have been mediated by VCAM-1 and VLA-4 in our experimental models. By using CD133$^+$ cells labeled with nanoparticles of iron oxide and MRI, it was possible to demonstrate the presence of migrated stem cells into the muscle after intra-arterial injection. In addition, muscle swimming exercise increased the percentage of human dystrophin–positive myofibers by 4-fold in all observed muscle tissues, documenting that exercise increases the recruitment of CD133$^+$ cells into the dystrophic muscle. The increase of CD133$^+$ recruitment after exercise was also confirmed by microfil perfusion. To demonstrate the importance of VCAM-1 in the recruitment of human circulating CD133$^+$ cells, we performed blocking experiments with radiolabeled cells. We registered a marked reduction of approximately 10-fold in the radioactivity in the muscle of dystrophic mice injected with anti–VCAM-1 mAb before CD133$^+$ cell administration. These results clearly demonstrate that VCAM-1 blockade prevented CD133$^+$ accumulation in the dystrophic muscle and that the VCAM-1/VLA-4 adhesion receptor pair has a critical role in the recruitment of stem cells to dystrophic muscle vessels. Our results are supported by recent studies showing that VCAM-1 acts as an "endothelial homing molecule" with a role in the recruitment of stem cells in

inflamed central nervous system.[13] However, further studies are needed to enhance the migratory ability of $CD133^+$ cells and to understand other mechanisms of stem cell homing, such as chemokines and chemokine receptors controlling integrin activation, leading to arrest in dystrophic vessels and chemotaxis in the damaged muscle. In conclusion, our results show that the induction of VCAM-1 expression on the dystrophic muscle endothelium represents a key mechanism of delivery of $CD133^+$ cells, allowing for improvement in potential therapy for muscular dystrophy based on the intra-arterial administration of stem cells.

References

1. Torrente Y, Belicchi M, Sampaolesi M, et al. Human circulating AC133(+) stem cells restore dystrophin expression and ameliorate function in dystrophic skeletal muscle. J Clin Invest. 2004; 114:182-195.
2. Sampaolesi M, Torrente Y, Innocenzi A, et al. Cell therapy of alpha-sarcoglycan null dystrophic mice through intra-arterial delivery of mesoangioblasts. Science. 2003;301:487-492.
3. Mazo IB, Gutierrez-Ramos JC, Frenette PS, Hynes RO, Wagner DD, von Andrian UH. Hematopoietic progenitor cell rolling in bone marrow microvessels: parallel contributions by endothelial selectins and vascular cell adhesion molecule 1. J Exp Med. 1998;188:465-474.
4. Piccio L, Rossi B, Scarpini E, et al. Molecular mechanisms involved in lymphocyte recruitment in inflamed brain microvessels: critical roles for P-selectin glycoprotein ligand-1 and heterotrimeric G(i)-linked receptors. J Immunol. 2002;168: 1940-1949.
5. Battistini L, Piccio L, Rossi B, et al. $CD8^+$ T cells from patients with acute multiple sclerosis display selective increase of adhesiveness in brain venules: a critical role for P-selectin glycoprotein ligand-1. Blood. 2003;101:4775-4782.
6. Lawrence MB, Springer TA. Leukocytes roll on a selectin at physiologic flow rates: distinction from and prerequisite for adhesion through integrins. Cell. 1991;65:859-873.
7. Laudanna C, Constantin G. New models of intravital microscopy for analysis of chemokine receptor-mediated leukocyte vascular recognition. J Immunol Methods. 2003;273:115-123.
8. Gianolli L, Dosio F, Matarrese M, et al. ^{99m}Tc-2GAM: a tracer for renal imaging. Nucl Med Biol. 1996;23:927-933.
9. Jendelovà P, Herynek V, De Croos J, et al. Imaging the fate of implanted bone marrow stromal cells labeled with superparamagnetic nanoparticles. Magn Reson Med. 2003;50:767-776.
10. Sykova E, Jendelova P. Magnetic resonance tracking of implanted adult and embryonic stem cells in injured brain and spinal cord. Ann N Y Acad Sci. 2005;1049:146-160.
11. Butcher EC, Picker LJ. Lymphocyte homing and homeostasis. Science. 1996;272:60-66.
12. Ley K, Kansas GS. Selectins in T-cell recruitment to non-lymphoid tissues and sites of inflammation. Nat Rev Immunol. 2004;4:325-335.
13. Pluchino S, Zanotti L, Rossi B, et al. Neurosphere-derived multipotent precursors promote neuroprotection by an immunomodulatory mechanism. Nature. 2005;436:266-271.